Regional Manifestation of the Widespread Disruption of Soil-Landscapes by the 4 kyr BP Impact-Linked Dust Event Using Pedo-Sedimentary Micro-Fabrics

Marie-Agnès Courty, Alex Crisci, Michel Fedoroff, Kliti Grice, Paul Greenwood, Michel Mermoux, David Smith, and Mark Thiemens

Abstract The co-occurrence of a sharp dust peak, low lake levels, forest reduction, and ice retreat at ca. 4-kyr BP throughout tropical Africa and West Asia have been widely explained as the effect of an abrupt climate change. The detailed study of soils and archaeological records provided evidence to re-interpret the 4 kyr BP dust event linked rather to the fallback of an impact-ejecta, but not climate change. Here we aim to further investigate the exceptional perturbation of the soil-landscapes widely initiated by the 4 kyr BP dust event. Results are based on soil data from the

Marie-Agnès Courty
UMR 5198, CNRS-IPH, Centre Européen de Recherches Préhistoriques,
Avenue Léon-Jean Grégory, 66720 Tautavel, France, e-mail: courty@tautavel.univ-perp.fr

Alex Crisci
CMTC INP, 1260 rue de la Piscine, BP 75, 38402 Saint Martin d'Hères, France

Michel Fedoroff
Laboratoriy of Electrochimie & Chimie analytique, ENSCP,
11 rue Pierre et Marie Curie, 75231 Paris, France

Kliti Grice
Department of Applied Chemistry, Curtin University of Technology,
GPO Box 1987, 6845 Perth, Australia

Paul Greenwood
Department of Applied Chemistry, Curtin University of Technology,
GPO Box 1987, 6845 Perth, Australia

Michel Mermoux
LEPMI-ENSEEG, Domaine Universitaire, BP75, 38042 Saint-Martin d'Hères, France

David Smith
Labority of LEME/Nanoanalysis, MNHN, Laboratoire de Minéralogie,
61 rue Buffon, 75005 Paris, France

Mark Thiemens
Department of Chemistry and Biochemistry, University of California,
San Diego 92093-0352, USA

S. Kapur et al. (eds.), *New Trends in Soil Micromorphology*,

eastern Khabur basin (North-East Syria), the Vera Basin (Spain), and the lower Moche Valley (West Peru) compared with a new study at the reference site of Ebeon (West France). The quality of the 4 kyr BP dust signal and the related environmental records are investigated through a micromorphological study of pedo-sedimentary micro-fabrics combined with SEM-microprobe, mineralogical, and geochemical analyses.

In the four regions studied, the intact 4 kyr BP signal is identified as a discontinuous burnt soil surface with an exotic dust assemblage assigned to the distal fallout of an impact-ejecta. Its unusual two-fold micro-facies is interpreted as (1) flash heating due to pulverization of the hot ejecta cloud at the soil surface, and (2) high energy deflation caused by the impact-related air blast. Disruption of the soil surface is shown to have been rapidly followed by a major de-stabilisation of the soil cover. Local factors and regional settings have exerted a major control on the timing, duration, and magnitude of landscape disturbances. Studies showed how a high quality signal allows to discriminate the short-term severe landscape disturbances linked to the exceptional 4 kyr BP dust event from more gradual environmental changes triggered by climate shift at the same time.

Keywords Impact-ejecta · soil surface · dust · flash heating · air blast · soil destabilization

1 Introduction

High resolution records in ice, marine and lake cores show recurrent climate shifts of global extent, possibly with millennial scale cyclicity throughout the Holocene (Alley et al. 1993, Bond et al. 1999, Mayewski et al. 2004). The 4000 yr BP dust event first identified in soils of northern Mesopotamia (Weiss et al. 1993), later traced as a sharp dust peak in the Arabian Gulf (Cullen et al. 2000), in Huascaran ice cores from the Andes of northern Peru, and a thick dust layer in the Kilimanjaro ice (Thompson et al. 2002) is commonly assigned to the millennial cyclicity (de Menocal 2001). The inferred 300-year long drought was concluded to have forced the abandonment of agricultural settlements in northern Mesopotamia (de Menocal 2001, Weiss and Bradley 2001). Major societal disturbances apparently synchronous around this period of time throughout the Mediterranean basin and Asia were attributed to the severe decrease of annual precipitation, widespread cooling, forest removal, and drastic flow reduction of major rivers broadly coincident with the radical increase in airborne dust (Weiss and Bradley 2001, Wang et al. 2004). This short-lived shift would have been triggered by large scale changes in the ocean-atmosphere-vegetation boundary conditions, comparable in amplitude to the global aridification of the Younger Dryas (12 900-11 500 yr BP), (Cullen et al. 2000, Weiss 2001).

Recently, the intriguing dust peaks were suggested to represent regional manifestation of the 4 kyr BP pronounced environmental shift (Marchant and Hooghiemstra 2004).

Combined microscopic and geochemical investigations from a wide range of soil-sedimentary, and archaeological sequences in the Near East have allowed us to interpret the 4 kyr BP dust-event as the fallout of a distal impact-ejecta rather than a sudden drought (Courty 1998, 2001, 2003). Its exotic petrography with geochemical anomalies, and the related unusual pedo-sedimentary micro-fabrics helped us to link the fallout of the far-traveled dust with high temperature effects at the soil surface and violent deflation of surface horizons by high speed winds. We suggested the micro-debris fallout and the related manifestations to possibly trace effects of the distal dispersion of impact-ejecta.

Our objectives were to: (1) consolidate the widespread extent of the exceptional 4 kyr BP dust event based on soil sequences from contrasting geomorphic, geologic, and climatic settings; (2) compare the regional manifestations of the timing, spatial variability and controlling factors of soil disturbances, which started with the 4 kyr BP dust event; and (3) further elucidate the confusing resemblance of this exceptional dust event with a climate-triggered drought.

2 Materials and Methods

2.1 Site Selection

Soil anomalies at about 4 kyr BP were searched on soil sequences of the eastern Khabur basin (north-east Syria, Fig. 1a), the Vera basin (Spain, Fig. 1b) and the lower Moche valley (Peru, Fig. 1c). This focus is part of the interdisciplinary projects studying the evolution of the Holocene soil-landscapes with respect to anthropogenic forcing and climate changes (Courty 1994, Courty et al. 1995). A unique perturbation of soil-landscapes throughout the Holocene was identified from a stratigraphic discontinuity showing similar unusual burnt facies in all three regions.

Absolute radiometric dating and archaeological data were used to independently confirm attribution of the burnt facies to the 4 kyr BP event. At Ebeon (western France, Fig. 1d) the unique section exposed during the excavation of a Middle Neolithic ditch displays an unusual fired-strata dated at ca. 4 kyr BP, incompatible with a human activity but strongly resembling the 4 kyr BP burnt soil surface signal.

2.2 The Eastern Khabur Basin (North-East Syria)

The eastern Khabur basin (north-east Syria) forms a gently undulated flood plain within an endoreic alluvial basin under a semi-arid Mediterranean climate. Soil

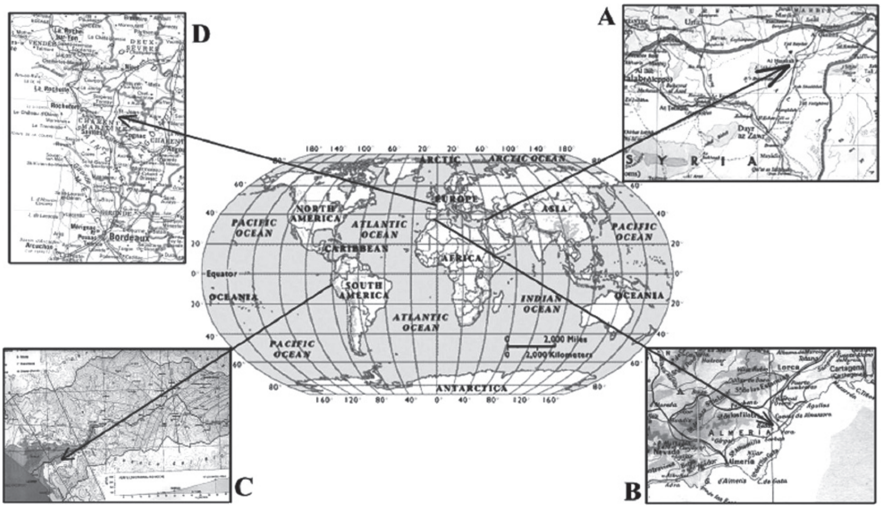

Fig. 1 Location of the studied regions: **(a)** Eastern Khabur basin (northeast Syria); **(b)** Vera basin (Spain); **(c)** lower Moche valley (Peru); **(d)** site of Chemin Saint-Jean at Authon-Ebeon (Charente Maritime, France)

landscapes have progressively aggraded since the last phase of channel incision at the end of the Pleistocene (Courty 1994) and supply of airborne dust from distant sources and nearby regions. The cumulative soil sequence offers a nearly continuous record of the Holocene climate fluctuations and a well-preserved signal of the 4 kyr BP burnt surface that can be spatially traced (Fig. 2a).

The related sequences display successive pedo-sedimentary units with characteristics of Calciorthids and Camborthids (Soil Survey Staff 1993). The weakly expressed horizon boundaries mostly result from gradual structure changes and abundance of pedogenic carbonates (Gaffie et al. 2001). Clayey to loamy-clay, homogeneous parent materials with 30–40% total carbonate content, have a clay mineral assemblage dominated by palygorskite and smectite.

2.3 The Vera Basin (Spain)

The Vera basin located in the most arid zones of southeast Spain is part of the transcurrent shear zone of Palomares. The combined effects of its tectonic instability, climate fluctuations and sea level changes have maintained a recurrent erosional crisis (Courty et al. 1995). Since the last phase of active tectonic uplift during the Middle Pleistocene (Ott d'Estevou et al. 1990, Zazo et al. 1993), the Vera basin has suffered from recurrent erosion. Devonian/Permian limestones and Triassic marls with deep gullied narrow basins (Fig. 3) are common. Soils are also highly eroded in the mid-altitude zones with extensive bad-lands developed from the Neogene marls and turbidites, and patches of Plio-Pleistocene conglomerates.

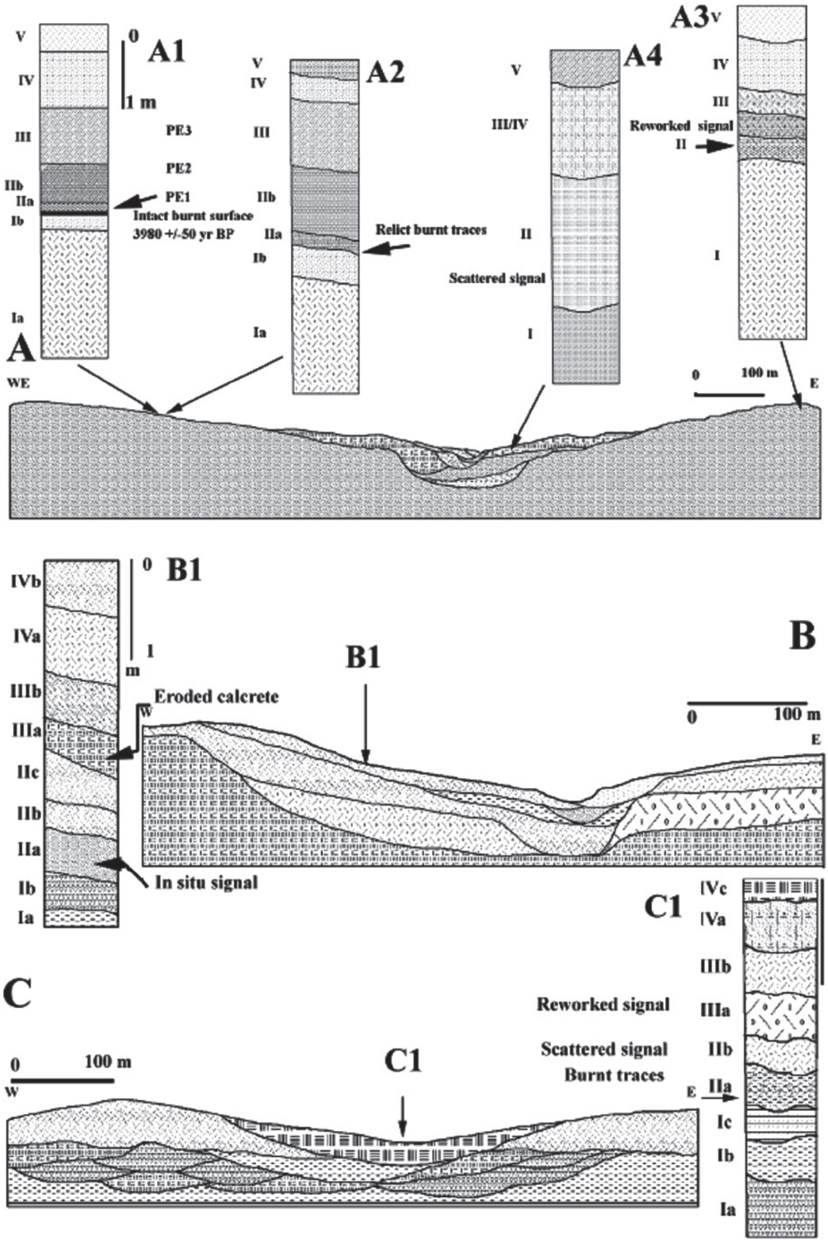

Fig. 2 Soil sequences in the eastern Khabur basin (north-east Syria). **(a)** undulated flood plain of Wadi Jarrah: (**a**1) intact 4 kyr BP signal (**a**2), well preserved primary signal (IIa), fossilised by rapid burial (IIb); (**a**3) reworked primary signal (II); (**a**4) secondary signal (II) (II) in the lower flood plain. **(b)** Flood plain of wadi Rijlet Aaoueji: (**b**1) thick 4 kyr BP signal along the slope (II); post-event erosion of the calcrete (IIIa). **(c)** southern Radd basin: (**c**1) shift at 4 kyr BP (IIa) from alluvial discharge in a wide endoreic basin (Ia to Ic) to dust deposition in a closed depression (IIIa to IVc)

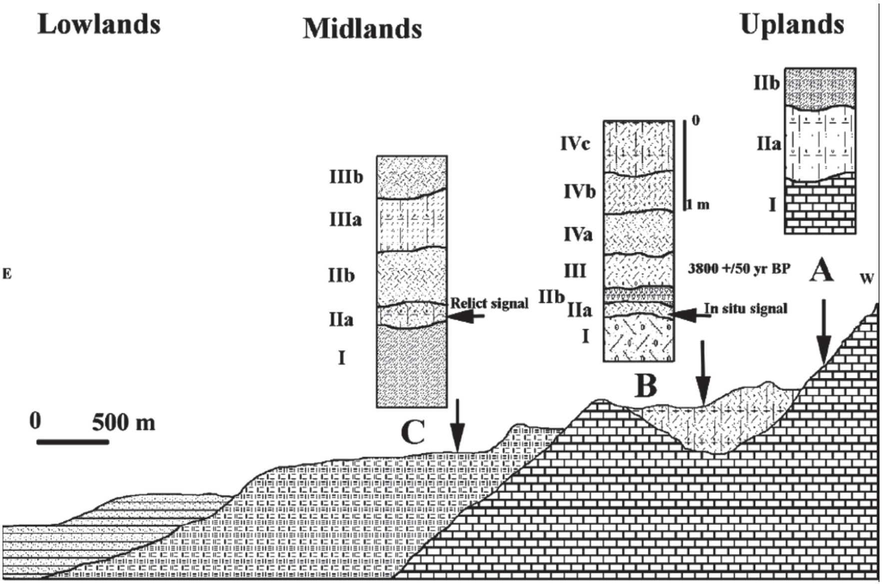

Fig. 3 Sections in the lower Aguas valley, Vera basin (Spain): **(a)** Highly eroded soil sequence in a dolina of the Permian limestone; **(b)** Rambla Añofli soil sequence with an intact 4 kyr BP burnt surface (IIa & IIb) sealed by the schistaceous mudflow (III); **(c)** Soil sequence on Miocene gypsiferous marls (I) showing a relict 4 kyr BP signal (IIa) preserved by erosion of the Gysiorthids (IIb)

The lowlands delineated by relicts of Pleistocene coarse-textured terraces, are presently flowed by three meandering channels, the Aguas, the Antas and the Almanzora. Tracing the 4 kyr BP fired strata in the lower alluvial plain was a delicate task due to the scarcity of natural exposures, the lack of reliable dating and the high amount of silting caused by re-activated erosion of the Neogene marls with modern agriculture.

2.4 The Lower Moche Valley (Peru)

The study area along the lower Moche valley belongs to the hyper-arid North Peruvian coast. In the flat littoral fringe, the Moche river is widely braided and weakly incised. The upper flood plain is blanketed by undulating sand dunes formed from deflation of the continental plateau during the late Pleistocene marine transgression,

The leveled pampas formed of complex sedimentary deposits of marine, eolian, colluvial-alluvial, and alluvial origin are delineated by Cretaceous granodiorite outcrops (Fig. 4). The Moche hydrographic regime is controlled by seasonal variations of heavy rainfall over the upper catchment basin in the Occidental Cordillera of the Andes at 4000 m altitude. Turbulent flooding during the recurrent El Niño episodes

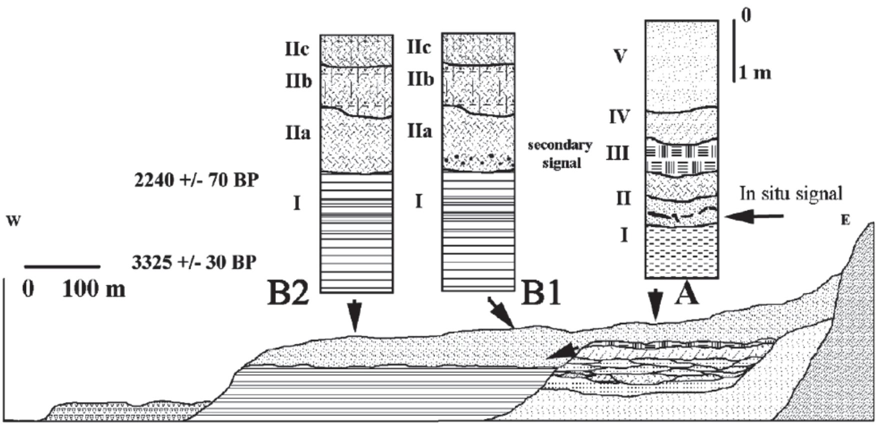

Fig. 4 **(a)** Soil sequences in the lower Moche valley (Peru). (I) Fluvisols on braided channel deposits, (II) Entisol on aeolian sand associated to the 4 kyr BP burnt soil surface, (III) the mudflow deposit. **(b)** Micro-stratified flood deposits with cyclical wild fires (I); B1: secondary 4 kyr BP signal eroded from the former river bank (IIa), not present in B2

leads to severe devastation of the lower flood plain, as illustrated by the major soil loss, following the last 1998 El Niño event.

2.5 The Neolithic Ditch Fill at Chemin Saint-Jean, Authon-Ebeon (Charente-Maritime, France)

The ditch dug into late Jurassic clay-rich limestone occupies a high position in the weakly undulated landscape. The Regosol (IUSS-WRB 2006) of about 50 cm thick shows only weak horizonation due to deep ploughing up to the underlying limestone. The distinct burnt layers contrast from the underlying and overlying filling units by their fine texture and low amount of coarse limestone fragments derived from the collapse of the unstable ditch sides (Fig. 5).

2.6 Analytical Procedure

The stratigraphical discontinuity of the 4 kyr BP event as previously defined in north-east Syria (Courty 1998, 2001) was detected in the field based on anomalies of colour, structure and texture, and patterns of burnt traces (Courty et al. 2005, 2006). The quality of the 4 kyr BP signal was then established from the compositional range, morphology and particle size distribution of the diagnostic micro-debris as given by successive test sampling on large amounts of bulk sediments collected along the stratigraphic discontinuities.

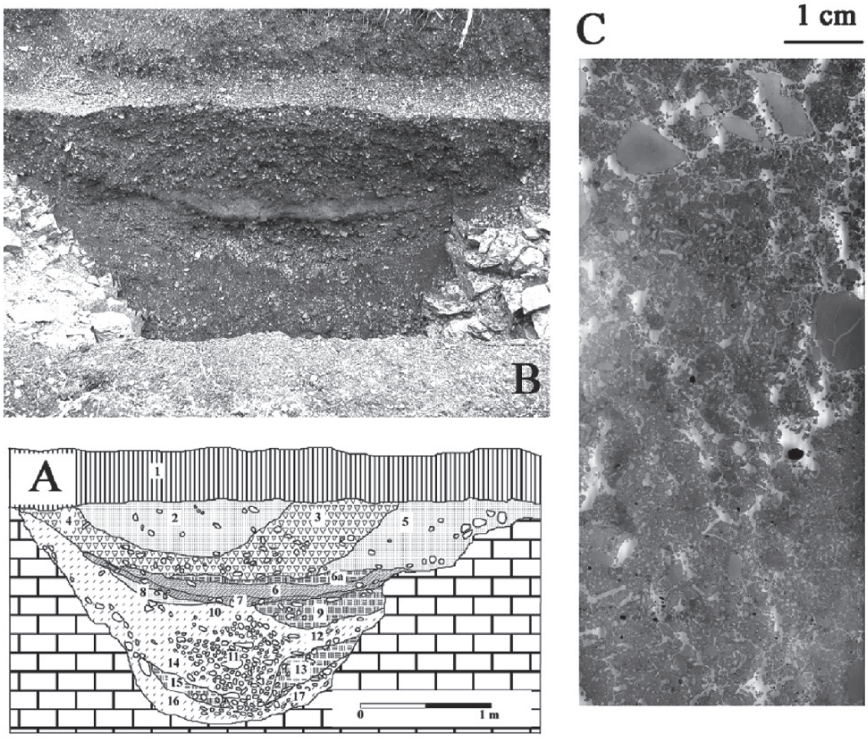

Fig. 5 Section in the Neolithic ditch fill at Chemin Saint-Jean, Authon-Ebeon (Charente-Maritime, France). **(a)** strata 17 to 8: collapse of the ditch talus; strata 6 & 7: anomalous units bearing the 4 kyr BP signal; strata 5 to 2: upper fill; strata 1: ploughed soil horizon. **(b)** dark brown strata in the field (7: FIa) overlaid by the reddish strata (6a and 6: FIb). **(c)** View in thin section of the homogeneous red strata (6) (see Fig. 8g for detailed view)

The spatial extent and micro-stratigraphical pattern of the intact 4 kyr BP signal were controlled through careful exposure of the host burnt surface. Undisturbed blocks and a series of refined bulk samples extracted from each micro-strata were collected throughout the exposed burnt surface. Continuous vertical columns of undisturbed samples were also collected at locations showing the most complete micro-stratigraphical succession. Thin sections were prepared from the blocks and studied under the petrographic microscope following the principles and terminology adapted from sedimentary petrography (Humbert 1972) and soil micromorphology (Bullock et al. 1985, Courty et al. 1989). A preliminary petrographical classification of the 4 kyr BP coarse fraction assemblage was established under the binocular microscope. XRD, isotope geochemistry, SEM/EDS, EPMA, TEM, GC-IR-MS and Raman spectrometry were used to characterize components on the 4 kyr BP signal. Thin sections were prepared from both selected areas of the large impregnated blocks and from a selection of extracted coarse grains for SEM and microprobe analyses.

3 Characterization of the 4 kyr BP Signal

3.1 Diagnostic Tracers of the 4 kyr BP by Petrographic Assemblage

In the four studied regions, a spatially irregular stratigraphic discontinuity with similar unusual burnt traces, in particular patches showing a completely incinerated surface horizon, is identified associated to a similar assemblage of exotic micro-debris (see Figs. 2a1, 3b, 4a, 5b), (Courty 2003, Courty et al. 2006). For the four situations encountered, attribution of these anomalies to the 4 kyr BP event was based on the common petrographic dust assemblage and age estimate (3800–4200 yr BP uncal.) depending upon the absolute radiometric dating and locally available archaeological data (Burnez et Fouéré 1999, Courty 2003, Courty et al. 1995, 2005).

In contrast from the local sediments, the exotic micro-debris predominantly consist of particles between 100 and 400 μm, with rare occurrence of larger grains up to 7 cm. Finer particles are also abundant but more difficult to isolate because of the dilution in the local background. Based on repeated sampling, the dust components are shown not to form a distinct stratum but to occur as discrete concentrations within a few cubic centimetres, with rapid variations at short spatial scales in the nature and abundance of the exotic particles (Courty et al. 2005). A similar assemblage from the different localities (Fig. 6) was obtained from water sieving of some ten kilograms of bulk sediments from the distinctive burnt surface.

It comprises a full range of spherules, droplets, teardrops and dumbbells that are often welded, glazed vesicular beads with an irregular shiny, sub-metallic, greyish yellow surface spread with spherules, and grey vesicular fragmented beads (Figs. 6a,b,c, and 7d). Angular fragments of white, whitish blue, dark brown and black, vesicular glass are common together with carbonate beads, often with metallic mounds lining the vesicles (Fig. 6e,g,h).

Vesicular beads showing partial devitrification and igneous-like coarse-textured re-crystallization are frequent (Fig. 6d). Black vesicular carbonaceous grains are common, and green carbonaceous materials associated to metallic deposits always occur as individual fibres, intricate vesicular fibres and angular fragments, together with metal-associated bright yellow and blue grains, translucent grains both as flakes and as blocky grains, and metallic particles present as platy ribbon, flakes, thin films, angular grains and spherules (Fig. 6f).

Various types of sulphates (Ca, Mg, Sr, Ba), and chlorides (K, Na) occur together with iron sulphide, phosphide, phosphate, and silicon-phosphate either as inclusions within the glassy debris (Fig. 6c) or as individual grains (Courty et al. 2005, 2006). The debris assemblage also comprises dumbbell millimetre-sized reddish brown to dark brown, carbonaceous aggregates with highly resistant, charred fine roots (Fig. 7a,b,c).

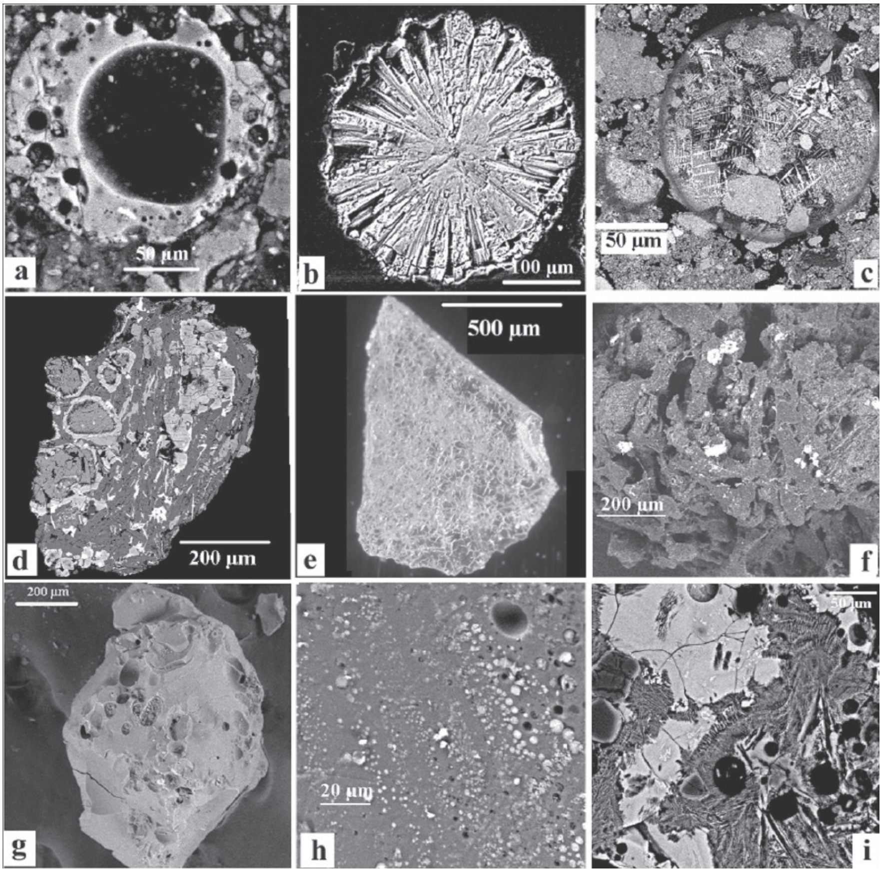

Fig. 6 The 4 kyr BP impact-debris assemblage: **(a)** Silicic spherical droplet. NE Syria, Tr.A1, IIa. SEM-BSE. **(b)** Heated re-crystallized foraminifera. NE Syria, Tr.A1, IIa. SEM-BSE. **(c)** KCl carbonaceous spherule. Moche valley, Peru, Tr. A, II. SEM-BSE. **(d)** Recrystallized igneous clast. NE Syria, Tr.A1, IIa. SEM-BSE. **(e)** C-rich silicic glass. Vera basin, Tr. B, IIa. **(f)** Metal-rich green vesicular fibrous carbonaceous glass (Ag and Fe-Cr-Ni). Ebeon, France, unit 7. SEM-BSE. **(g)** Whitish blue silicic glass. Ebeon, France, unit 7. SEM-BSE. **(h)** Enlarged view of **(g)** showing carbon-rich nickel phosphide splash. SEM-BSE. **(i)** Finely imbricated glass phases from rapid quenching of incompletely melted silicic and carbonate precursors. SEM-BSE

3.2 Anomalous Micro-Facies of the Buried Burnt Soil Surface

The most striking anomaly of the burnt soil surface associated to the exotic micro-debris is the succession of a dark stratum at the bottom overlain by a reddish layer (Fig. 5b). This reversed microstratification in contrast to the thermal record of wild fires or anthropogenic hearths (Courty et al. 1989) reveals the occurrence of two different micro-strata under the petrographic microscope with distinctive anomalous micro-facies (FIa and FIb) and related micro-debris (Courty et al. 2006).

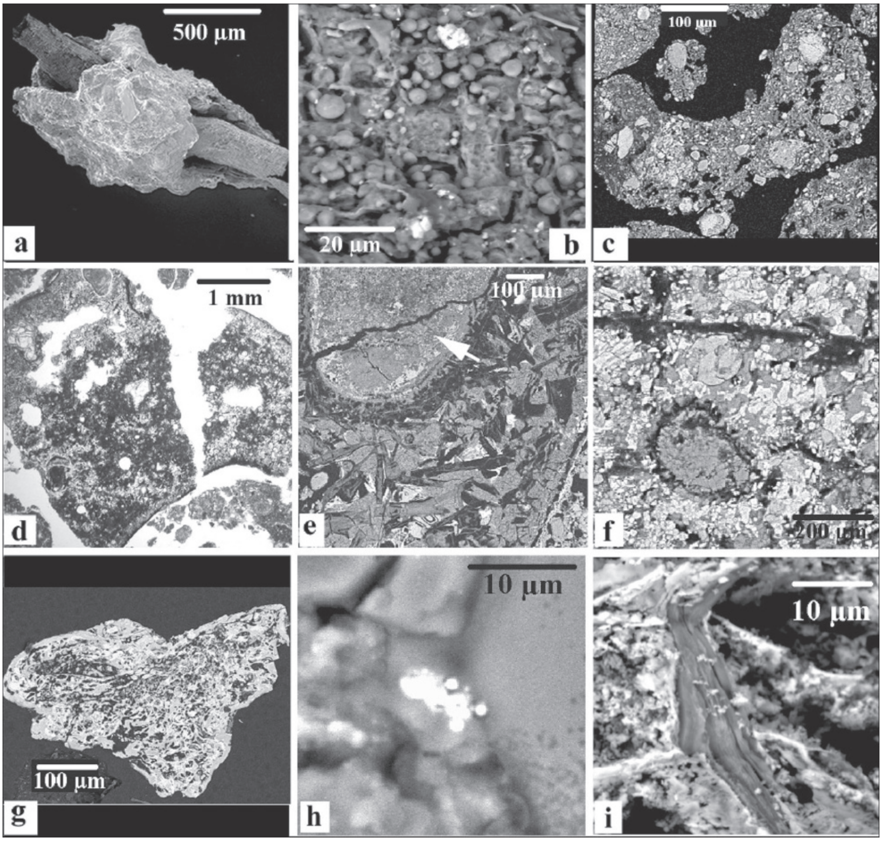

Fig. 7 Pulverisation of the hot ejecta cloud at the soil surface. (**a**) Charred fine root SEM-SE. Ebeon, France, unit 7. (**b**) Enlarged view showing pulverisation of carbonaceous micro-spherules, metal (bright particles) and glass micro-debris. SEM-BSE. Ebeon, France, unit 7. (**c**) Dumbbell carbonaceous aggregate. NE Syria, Tr.A1, IIa. SEM-BSE. (**d**) Vesicular glass bead. NE Syria, Tr.A1, IIa. SEM-BSE. (**e**) Enlarged view of (**d**): complex C-rich glass phases with a recrystallized CaCO3 clast (arrow). (**f**) finely cracked quartz and feldspar grains and the heat-transformed fine mass. (**g**) melted bone fragment showing injection of the metal-rich carbonaceous impact glass within the osteocytes. SEM-BSE. Ebeon, France, unit 7. (**h**) Silt-sized zircons-ZrSiO4– transformed into baddelyite-ZrO2 in the impact glass. SEM-BSE. Ebeon, France, unit 7. (**i**) Flow glass injected within the host soil materials. SEM-BSE. Ebeon, France, unit 7

The lower micro-facies (FIa) consists of a few millimetre to a few centimetre thick ashy unit formed of the incinerated original soil surface (Fig. 8b). The FIa on the undisturbed underlying horizon (Fig. 8a) displays an open packing of finely disrupted micro-aggregates with a darkened fine mass, associated to carbonised micro-rootlets, partially replaced by reddish iron oxides (Fig. 8c,d,h). In general, the birefringence of the fine mass in the burnt aggregates does not appear significantly modified as compared to the underlying weakly burnt aggregates.

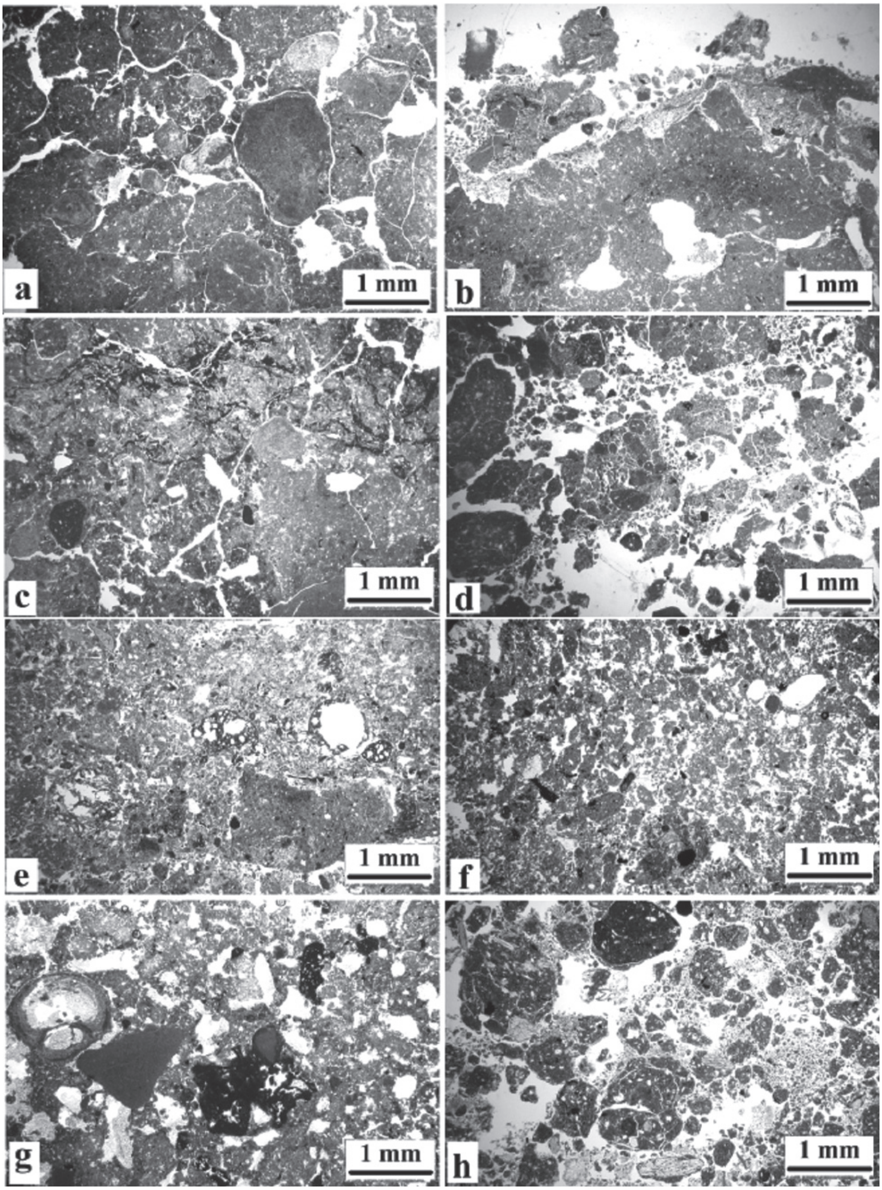

Fig. 8 Diagnostic microfabrics of the 4-kyr BP event. **(a)** Pre-event well structured soil. NE Syria, Tr.A1, Ia/Ib, PolM, PPL. **(b)** Calcinated vegetation, FIa microfacies. NE Syria, Tr.A1, IIa, PolM, PPL. **(c)** FIa microfacies: in situ carbonised rootlets. NE Syria, Tr.A1, IIa, MPol, PPL. **(d)** FIa microfacies: open packing of finely-disrupted heated micro-aggregates. NE Syria, Tr.A1, IIa, MPol, PPL. **(e)** FIa microfacies: impact glass beads within the host soil surface. NE Syria, Tr.A1, IIa, MPOl, PPL. **(f)** FIb microfacies: loose air-transported biogenic aggregates. NE Syria, Tr.A2, IIa, MPol, PPL. **(g)** FIb microfacies: air-transported biogenic aggregates, limestone clasts and burnt soil aggregates. Ebeon, France, unit 6 bottom, MPol, PPL. **(h)** FIa microfacies: loose heated micro-aggregates. Vera basin (Spain), Tr.B, IIa, MPol, PPL

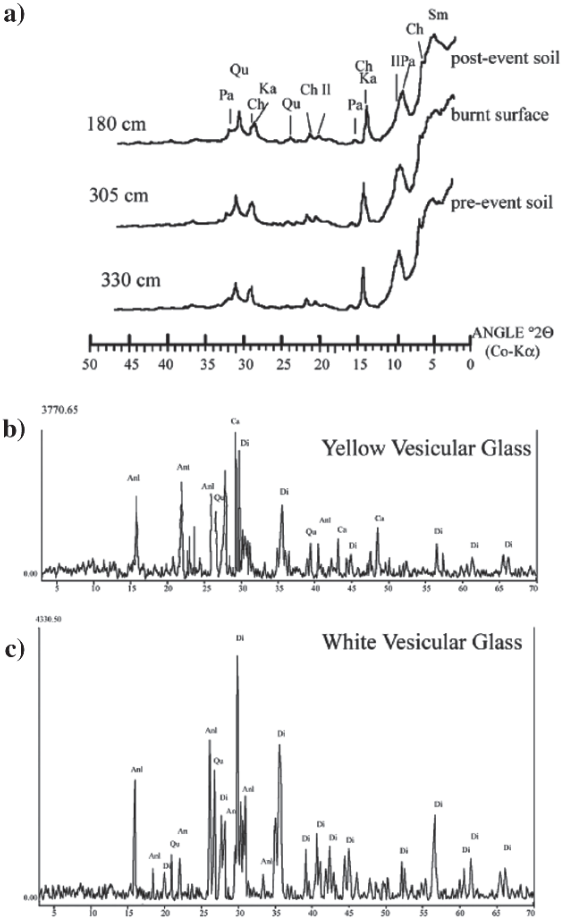

Fig. 9 **(a)** X-ray diffraction analysis, Leilan Tr. A1, NE Syria: moderate heating in the 4 kyr BP burnt surface (305 cm) as compared to the underlying soil horizon (330 cm) and the overlying soil unit (180 cm). **(b)** & **(c)** Mixing of high temperature recrystallized minerals and exogenous detrital minerals in the impact glass: diopside (Di), analcime (Anl), anorthite (Ant), calcite (Ca) and quartz (Qu)

Evidence for an overall moderate heating is confirmed by X-ray diffraction that does not show the irreversible change of the clay fraction (Fig. 9a). The most exotic micro-debris occur either as randomly distributed individual grains in the packing voids, as minute particles stuck to the micro-aggregates and within the carbonised roots (Figs. 7a,i, and 8d,h). Local concentrations of vesicular glass bodies are associated with high temperature transformation of the embedding matrix (Figs. 7d, 8e, 12c), as indicated by the development of a poorly crystalline phase of the clay-rich and carbonate-rich fine mass. This is confirmed by the transformation into diopside of the original alumino-silicate as shown by X-ray diffraction (Fig. 9b,c), of heated sample at around 700–850°C temperatures (Heimann 1982).

Fine vesicularity in the host materials attached to the glazed beads associated to the destruction of the poorly crystalline carbonate attests to the in situ carbonate decomposition by the loss of CO_2, due to local heating at temperatures around 700°C (Fig. 7e). Morphological and geochemical evidence for the thermal alteration of the host materials at the contact with the exotic components indicate temperature elevation up to ca. 1200°C (Fig. 7e,f). In contrast, the presence of heat-decomposed silt-sized zircons within the glassy phases of the glazed beads (Fig. 7h) attests for their formation at temperatures from 1400 to 2000°C (Courty et al. 2006) based on experiments (Pavlik et al. 2001). The similar compositional range of the high temperature phases between the vesicular glass bodies from distant sites suggests an exotic origin from a common source (Table 1).

The Ca-rich flow glass pattern with micro-scale compositional heterogeneities (Table 1) resembles a rare type of impactite glass (See et al. 1998, Graup 1999). The coarse glass bodies would have formed within an impact ejecta cloud possibly by rapid quenching of incompletely melted source materials (Kieffer 1977, Kring and Durda 2002). Penetration within fine pores of the host materials with interaction limited to an interfacial layer suggests final pulverisation of highly viscous hot liquid materials at the soil surface.

The darkened micro-aggregates locally display heat-induced amorphisation and abundant glassy micron-sized exogenous minerals similar to the coarse vesicular bodies (Fig. 7i). Glassy particles associated to clusters of metal-rich carbonaceous micro-spherules also occur around the charred fine roots, and within the calcinated layer (Fig. 7a,b,c). These suggest penetration into the surface soils of a carbonaceous volatile-rich phase associated to the hot mineral debris, possibly in the form of condensed droplets (Fig. 7g) through rapid dehydration (Hubbert et al. 2006). This would have resulted in a decreased wetting-ability of micro-aggregates, thus explaining their resistance to water treatment (Fig. 7a).

The upper microfacies (FIb) consists of loosely-packed reddish brown to dark brown dumbbell-shaped micro-aggregates. They are morphologically similar to the darkened ones present in the underlying facies, and also contain micro-particles diagnostic of the 4 kyr BP assemblage. Although their shape is typical of a biogenic origin, their random packing and lack of linkage to biological channels indicate a transport from their primary position (Figs. 7c and 8f). The direct juxtaposition of domains showing various intensities of thermal alteration indicates mixing of the burnt surface materials.

The common coarse-sized vesicular exotic debris typical of the 4 kyr BP assemblage occur as distinct particles without signs of interaction with the host materials, whereas the other categories of exotic debris show evidence of surface abrasion by aeolian transport (Fig. 8g). Rock fragments of millimetre to centimetre size derived from the surroundings and also from more distant regions are common in all the dust assemblages studied. The upper microfacies (FIb) is, thus, interpreted to result from deflation by high energy hot air flow of the burnt soil surface bearing the pulverized hot debris. The direct stratigraphic continuity between the two microfacies and the lack of turbation of the incinerated burnt layer suggests the flash heating to have immediately been followed by violent wind swirls. The explosive

Table 1 Major element comparison.XRF data in wt% on bulk devritrified glass, bulk glasses and host soils

	Bulk devritrified glasses			Bulk glasses		Glass phases						Host soils		
	RGVG1 LHI95B	RGVG1 AID95C	RGVG1 AID95B	YVG1 PE00A	WVG1 EB00A	dbrG1 EBG1	ybrG1 EBG2	yg1 EBG2	yrG1 EBG2	wG1 EBG3	bWG1 EBG4	H8 LEI95	H8 AID95	H8 PE00
SiO_2	47.58	46.86	47.49	67.05	67.05	53.65	62.57	66.01	68.04	74.68	83.75	28.54	19.92	39.35
TiO_2	0.89	0.87	2.74	0.8	0.69	0.24	0.73	0.16	0.59	0.68	0.71	0.46	0.31	0.2
$A1_2O_3$	12.42	14.31	15.28	11.48	9.66	15.35	12.41	5.63	9.66	8.64	5.53	7.46	4.97	7.88
Fe_2O_3	6.76	7.12	12.41	4.7	2.92	10.13	2.86	2.22	7.38	3.79	1.9	3.87	2.61	6.71
MuO	0.12	0.1	0.16	0.09	0.07	<dl	<dl	<dl	<dl	<dl	<dl	0.04	0.03	0.28
MgO	4.9	5.43	6.51	1.91	1.8	1.01	2.46	9.13	0.47	1.09	2.17	2.9	2.21	1.18
CaO	17.73	18.81	10.39	4.44	10.97	17.63	11.5	11.3	3.36	2.35	1.67	26.57	35.22	22.29
Na_2O	1.66	1.16	3.1	4.82	1.08	1.08	2.83	1.66	2.4	1.68	1.74	0.12	<dl	1.36
K_2O	1.45	1.63	1.17	1.35	4.08	0.04	4.03	3.44	6.35	6.84	2.33	0.89	0.62	1.09
P_2O_5	0.52	0.41	0.41	0.97	0.66	0.79	0.38	0.38	1.72	0.11	0.1	0.09	0.08	0.46
LOI	5.14	3.13	0.26	2.25	0.89	<dl	<dl	<dl	<dl	<dl	<dl	29.03	33.8	19.08
Total	99.17	99.83	99.92	99.86	99.87	99.92	99.77	99.93	99.97	99.86	99.9	99.97	99.77	99.88

fragmentation of coarse ejecta masses could have triggered the hot air turbulence, thus producing at a small scale the expected effects of impact air blast (Kring 1997, Kring and Durda 2002).

3.3 Spatial Variability of the Primary 4 kyr BP Signal and Secondary Disturbances

The in situ 4 kyr BP burnt soil surface occurs as discrete patches over a few square meters, laterally merging to scattered burnt traces. The FIa/FIb micro-facies succession appears as relict micro-fabrics in the form of discrete carbonaceous micro-aggregates and heated biogenic aggregates (Fig. 7a,c). Compared to the complete two-fold burnt facies, the 4 kyr BP exotic particles are similar, but less abundant. The fresh aspect of the exotic debris suggests an intact 4 kyr BP signal, with minimal bias by post-depositional disturbances. Local variability of the dust assemblage reflects the erratic dispersion of the impact-debris, possibly linked to heterogeneities in the initial ejecta melt (Kring and Durda 2002).

The correlation between morphological changes of the 4 kyr BP exotic assemblage and the drastic alteration of the associated micro-fabrics are expressed by two types of distortion of the original signal by post-depositional processes. These refer to distinctive palaeo-environmental implications.

The first type displays a low amount of diagnostic particles, even when sorting a larger volume of soils, a lack of a continuum of particles from coarse to very fine sizes, and no stratigraphical discontinuity (e.g. Fig. 2, Tr. A3: II; Fig. 3, Tr. C: IIa). The rather fresh aspect of the grains, as well as the recognition in thin sections of the rare heated micro-aggregates, and the evidence of the intense bioturbation suggest the occurrence of an in situ reworking mostly by biological activity along the soil development over a short period of time.

The second type shows markers of the 4 kyr BP event in later deposits, in particular coarse vesicular glassy grains (Fig. 4, Tr. B1: IIa and Fig. 12g). Reworking is indicated by the absence of the diagnostic fine particles in the surrounding matrix and the lack of the distinctive micro-fabrics formed by the interaction of the intruding flow glass within the host materials. Considering their fragility, the source deposits with a nearly intact signal would occur in the local surroundings.

4 Recognition of Soil-Landscape Disturbances Following the 4 kyr BP Event

Although its characteristics vary according to the local climate and geomorphic factors, the impact-induced soil destabilisation appears as a unique combination of processes in contrast to the range of soil changes encountered during the previous six thousand years (Courty 1994, Courty et al. 1995).

4.1 The Post-Event Soil Record in the Eastern Khabur Basin (North-East Syria)

In the loamy lowlands of the N-E Syrian flood plain, the post-event pedo-sedimentary unit displays a spongy porosity typical of structural collapse, weak bioturbation, slight depletion of the calcitic fine mass, and lack of secondary carbonates. Coarse slaking crusts and dusty clay coatings rich in fine silt-sized clusters of carbonaceous spheroids, mineral spherules, and glass shards are common (Fig. 10a,c). Abraded heterogeneous particles typical of the 4 kyr BP assemblage are abundant. This high-energy erosion of the burnt soil surface indicates exceptional heavy rains immediately following the impact (Fig. 2, Tr. A1: IIa).

Water-transport and accumulation in micro-depressions of the exotic micro-debris suggests the rainfall increase to not have lasted more than a few months. The anomalous carbonate depletion not expected to occur under an arid Mediterranean climate expresses significant acidification, possibly triggered by the impact-induced changes in atmospheric chemistry (Toon et al. 1997). Acid rain would possibly result in from the production of nitrous oxides and other chemicals due to the injection in the upper atmosphere of carbon-rich aerosols (Toon et al. 1997). The incorporation of black carbon into the clay coatings (Fig. 10b) also suggests acidification by the carbonaceous aerosols remaining in suspension at great altitude before being washed by rainwater.

In the overlying unit, the upper part of the pedo-sedimentary horizon displays a gradual change to a fine textured deposit (Fig. 2, Tr. A1: IIb) with a vughy to fissural porosity, along with coarse-textured intercalations integrated to the dense fine mass (Fig. 10d). This trend attests for an overall decrease of heavy rainstorms, the persistence of fine rains favouring silting and water saturation, and of low evaporation as indicated by the lack of secondary carbonates.

Just above the marked decrease of coarse textural features, the excremental fabric with channel-like porosity and the fine-textured homogeneous micro-fabric indicate recurrent windstorms and persistent low evaporation with the re-establishment of a seasonal contrast (Fig. 10e).

In the overlying pedo-sedimentary unit, the decrease of silting, the development of a total excremental micro-fabric and re-activation of the carbonate redistribution (Fig. 2, Tr. A1: IV) indicate progressive stabilisation of soil-landscapes under a marked seasonal contrast, broadly similar to the pre-event conditions (Fig. 10h). Based on the chronological data, the impact-linked climate anomaly did not last more than one hundred years.

In shallow basins delineated by calcrete, the pedo-sedimentary layers directly linked to the 4 kyr BP event are sealed by lenses of weakly sorted, loose carbonate nodules (Fig. 10). The sheet-flow erosion of the calcrete that had remained stable since the Late Pleistocene attests for the exceptional violence of the runoff generated by the heavy rain showers immediately following the 4 kyr BP event (Fig. 2, Tr. B1: IIIa).

In the more arid areas, the 4 kyr BP event marks the contact between six thousand years of regular flooding and the establishment of endoreism. The few metres

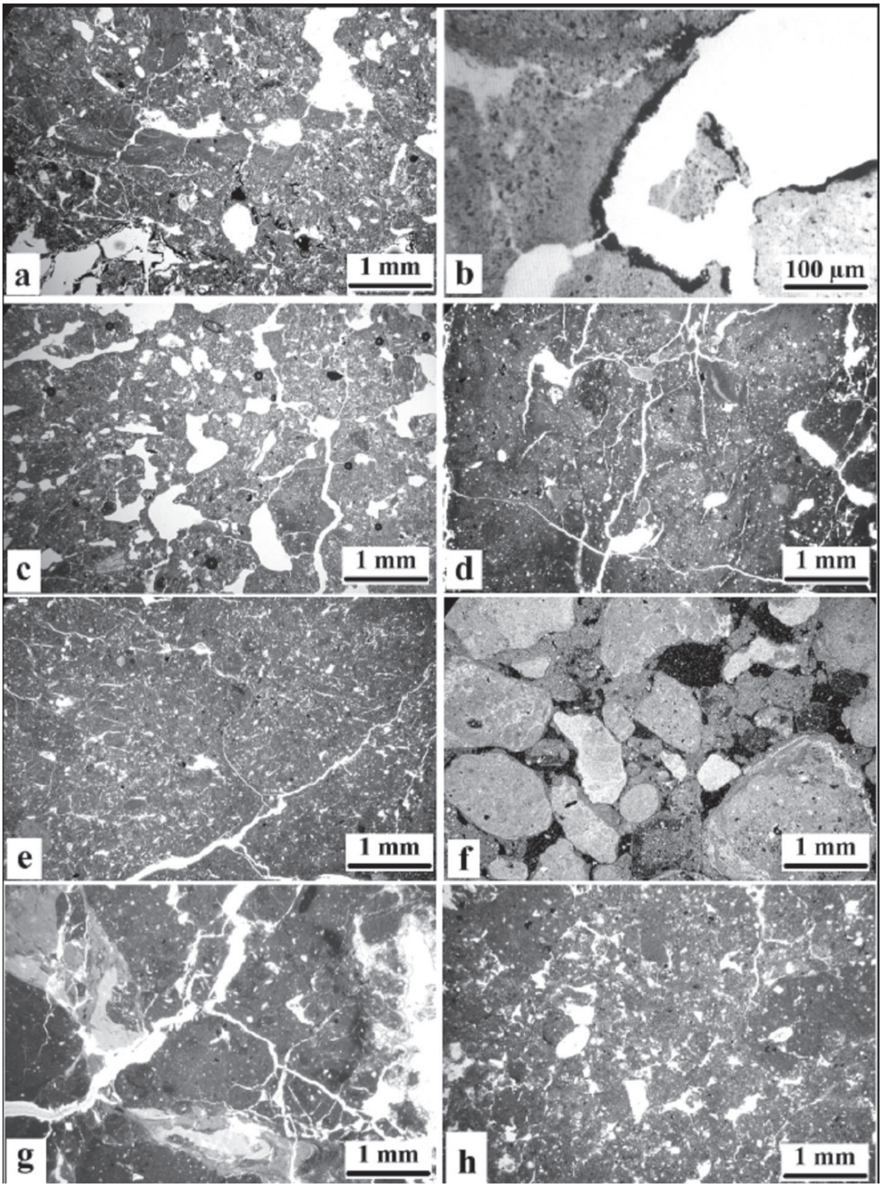

Fig. 10 Microfabrics following the 4-kyr BP event in the eastern Khabur basin (NE Syria). **(a)** Thick coarse textured slaking crusts. Tr.A1, IIb bottom, MPol, PPL. **(b)** Coarse clay coatings with rain-washed black carbon. Tr.A1, IIb bottom, MPol, PPL. **(c)** Spongy porosity, coarse clay coatings and intercalations. Tr.A1, IIb bottom, MPol, PPL. **(d)** Fissured to vughy microstructure with abundant intercalation and slaking crusts. Tr.A1, IIb bottom, MPol, PPL. **(e)** Fine textured micro-fabric. Tr.A1, IIb bottom, MPol, PPL. **(f)** Water-transported calcrete (see Fig. 2, tr. B1, IIIa). **(g)** Unusual thick clay coatings (see Fig. 2, tr. C1, IIb). (**h**) Well-developed excremental microfabric and diffuse calcitic impregnation. Tr.A1, III, MPol, PPL

thick succession of weakly bioturbated fine textured Entisols developed on the flood deposits with diffuse calcitic coatings merge to a fine-loamy Natraqualf with abundant textural features (Fig. 2, Tr. C1: IIa to IVc; Fig. 10g). Sudden salt accumulation well-expressed by the marked pH increase from 8.4 in the lower Entisols to 9.7 in the upper Natraqualf reflects the sudden disorganisation of drainage, most probably due to the massive re-mobilisation of dust with the maintenance of exceptional air turbulence.

4.2 The Post-Event Soil Record in the Vera Basin (Spain)

In the Vera basin, the filling of shallow dry valleys in the lower uplands (Fig. 3, Tr. B) above the 4 kyr BP burnt soil surface displays a heterogeneous micro-fabric. It comprises loosely-packed, heated reddish brown aggregates similar to the underlying unit, with disorganized earthworm pellets, abundant limestone fragments derived from the close outcrops, fragmented coarse-textured slaking crusts, and reworked pedogenic calcitic nodules (Fig. 11b).

The characteristics of the reworked pedogenic carbonates indicate an origin from the previously-developed Calciorthids and Camborthids formed on the uplands during the Holocene climatic optimum (Fig. 11a) at a period when the entire soil-landscape was broadly stable (Courty et al. 1995). The post-event pedo-sedimentary unit (Fig. 3, Tr. B: IIb) results from the severe erosion by high-energy runoff of the soil surface that recorded the 4 kyr BP event. Above, the sharp contact with a massive unit formed of fine-textured schistaceous sediments, with a flow structure and a vughy porosity, attests for liquefaction of the Precambrian schists by an exceptional mudflow immediately following the 4 kyr BP event (Fig. 11b,c). This severe mass movement of previously stable outcrops (Fig. 11a,b), attests for the considerable soil loss in the uplands due to the 4 kyr BP event (Fig. 3, Tr. B: IIb). The severe soil destabilisation is traced along the slopes of the midlands, down to the upper flood plain of the Aguas, although undisputable traces of the 4 kyr BP burnt surface are rare (Fig. 3, Tr. C: IIa).

In the overlying pedo-sedimentary units, the coarse texture, the micro-fabric heterogeneity, the poorly-developed structure together with the occurrence of slaking crusts attest for soil landscape instability up to the present time (Fig. 3, Tr. B: III to IVc; Fig. 11d). In contrast to the overall stability during the few thousand years, the severe soil loss linked to the 4 kyr BP event seems to have induced irreversible geomorphic changes in this highly dissected landscape.

The lack of interaction between the burnt soil layer and the overlying mudflow unit suggests a significant reduction of moisture retention of the heated soil surface, possibly due to the formation of hydrophobic compounds under fire (Almendros et al. 1990, Giovannini et al. 1983, Hubbert et al. 2006). The temporary decrease of soil wettability might have increased the risk of soil erosion as observed under wildfire conditions (Scott and Van Wyk 1990).

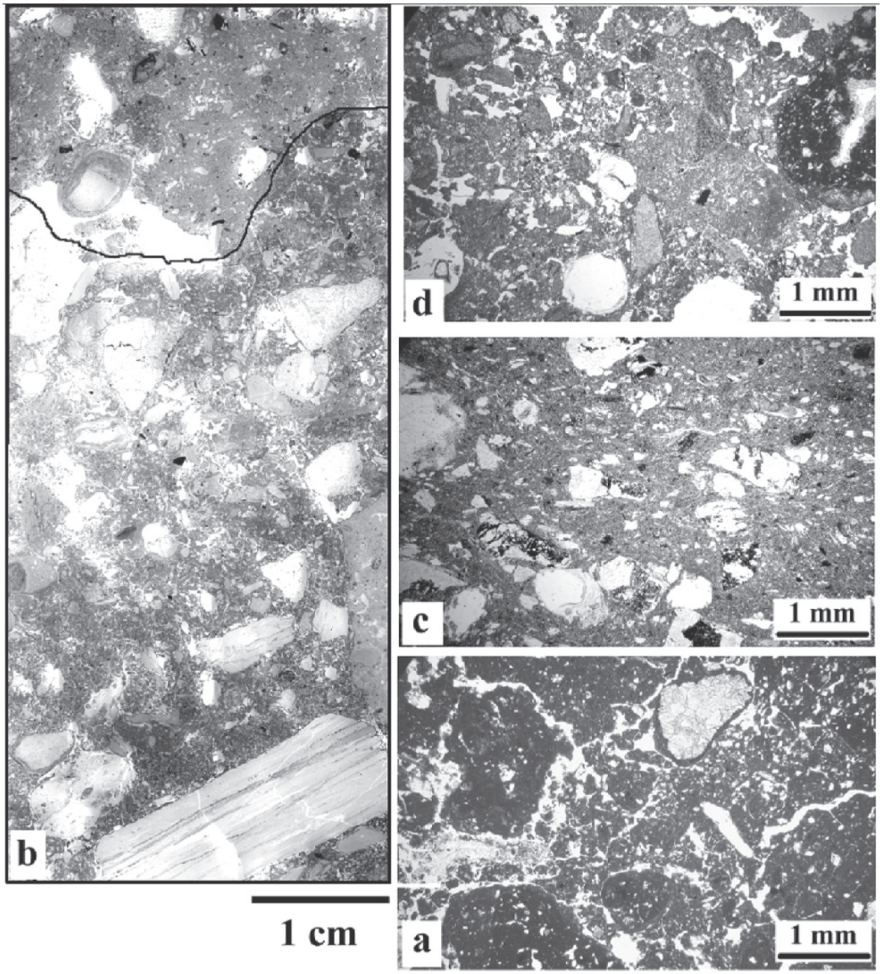

Fig. 11 Rambla Añofli, lower Aguas valley (Vera basin, Spain). Microfabrics related to the 4 kyr BP event (See Fig. 3, tr. B.). **(a)** well structured pre-event stable soil. Tr.B, I, MPol, PPL. **(b)** Sharp contact between the 4 kyr BP eroded surface soils and the subsequent schistaceous mudflow. Tr.B, IIb/III, MPol, PPL. **(c)** The fine textured schistaceous mudflow. **(d)** Limestone clasts, coarse textured slaking crusts and weakly developed excremental fabrics indicating maintenance of soil instability following the 4-kyr BP event. Tr.B, IVb, MPol, PPL

4.3 The Post-Event Soil Record in the Lower Moche Valley (Perou)

In the Moche valley, the burnt soil surface with the 4 kyr BP signal occurs within a thin blanket of structureless fine sand derived from aeolian reworking of the surrounding sand dunes (Fig. 4, Tr. A: II; Fig. 12b). The episode of sand remobilisation

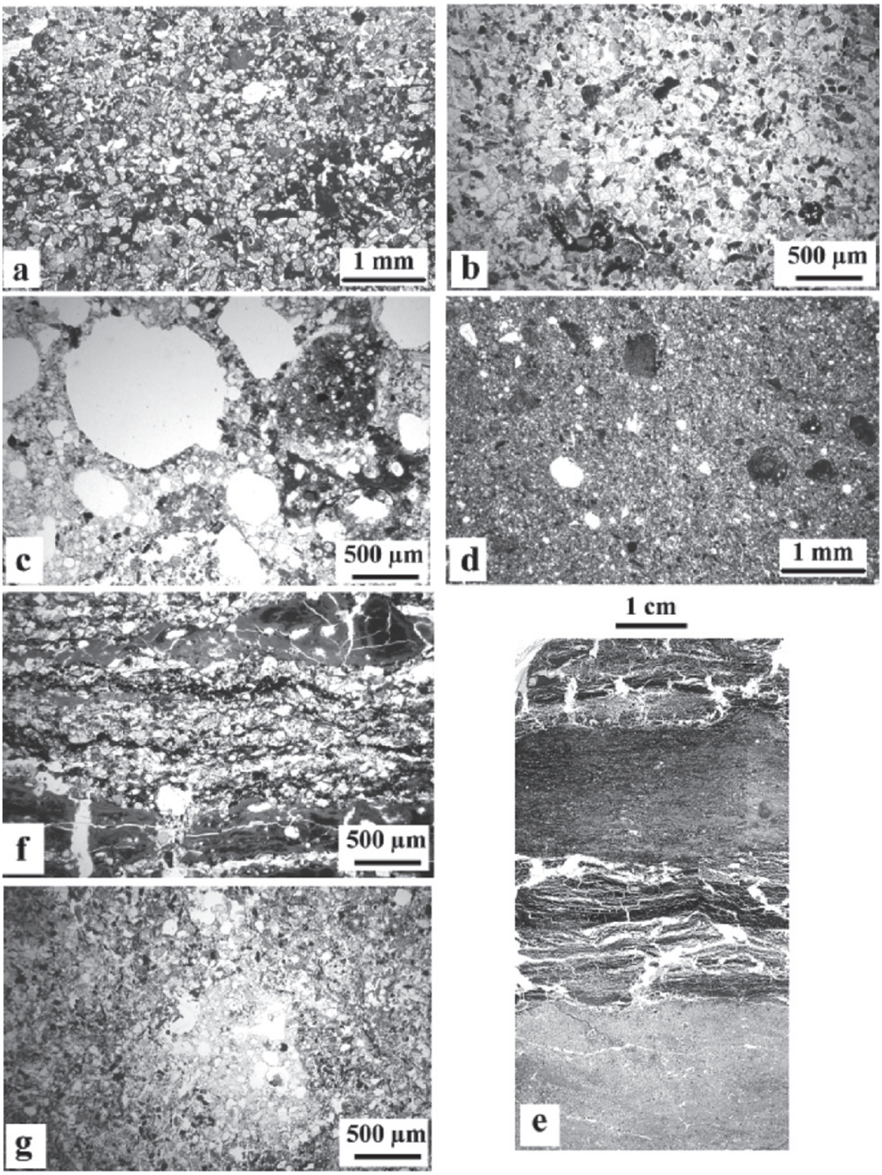

Fig. 12 Lower Moche valley (Peru). Microfabrics related to the 4 kyr BP event. **(a)** Well-structured pre-event soil with diffuse calcitic impregnation, sesquioxide hypocoatings. Tr. A, I, MPol, PPL. **(b)** Relict 4 kyr BP burnt soil surface within aeolian sands. Tr. A, II, MPol, PPL. **(c)** Impact glass beads within the heated host soil surface. Tr. A, II, MPol, PPL. **(d)** Massive fine textured flooded unit. Tr. A, III, MPol, PPL. **(e)** Finely laminated burnt organo-mineral deposits. Tr. B1, I, MPol, PPL. **(f)** Detailed view of **(e)** the clay and charred layers. **(g)** Impact glass beads in secondary position. Tr. B1, IIa bottom, MPol, PPL

is, however, not distinctive as compared to the recurrent instability of sand dunes recorded throughout the Holocene, linked to the inherent fragility of the coastal ecosystem under a hyper-arid climate.

The first and major environmental disturbance (Fig. 4, Tr. A: III; Fig. 12d) is recorded by the sharp depositional contact over the structureless fine sand of a massive fine-textured unit resulting from extensive flooding. This unit contrasts with the previous torrential discharge in braided channels of coarse sands, abundant gravels, and pebbles of local origin (Fig. 4, Tr. A: II; Fig. 12a). In the overlying massive clay-rich unit the abundance of illitic clay with a silt fraction derived from schistic materials indicates a substantial contribution from far-traveled components.

The resemblance of the clay-rich unit to the upstream valley deposits in the Andes at an altitude of about 4000 m incites to invoke a significant rainfall increase in the upper catchment valleys, immediately following the 4 kyr BP event. The related downslope mass movement of the soil caused the development of exceptional floods in the lower valleys, along with the erosion of the landscapes that had remained stable for more than five thousand years.

The following 1500 years (approx. 3700–2200 yr uncal. BP) were dominated by cyclical episodes of high energy alluvial reworking of the local sands and low energy regular flooding with deposition of micro-stratified fine textured alluvium (Fig. 4, Tr. B: I).

The micro-stratified sequence shows the alternation of the finely laminated sandy silt, deposited by gentle flooding, and finely laminated organo-mineral deposits rich in charred remains and burnt aggregates (Fig. 12e,f). This evolution suggests the maintenance throughout the year of the marshy conditions in the lower valley allowed by regular flooding from the upstream basin, episodically interrupted by wildfires during recurrent drought. After this episode of geomorphic stability, a new phase of channel incision eroded most of the previously formed flood plain when the torrential alluvial regime with recurrent exceptional El Niño episodes was re-established (Fig. 4).

Our interpretation of the existence of more humid conditions in the lower Moche valley at around 4 kyr BP seems to be in agreement with the increased precipitation known to have occurred from about 4000 yr BP throughout South America as indicated by the higher lake levels (Marchant and Hooghiemstra 2004).

5 Discussion

The synchronous occurrence in distant regions of the unique 4 kyr BP exotic assemblage with similar anomalous soil micro-fabrics suggests the possibility of a common trigger with widespread effects. The glass components have no equivalent in volcanic or anthropogenic by-products but have characteristics resembling impact glass.

In the four sites studied, mixing of the exotic micro-debris with remobilised dust derived from the local soils attests for violent air turbulence directly linked to the fallout of the impact-ejecta. The heterogeneity of the impact-products dispersion explains the spatial variability at local to regional scales of the dust-accumulation and the related micro-fabrics. The timing of the dust event related to the impact-pulverisation process at the ground surface appears abrupt and rather short from the succession of the pedo-sedimentary micro-fabrics, as predicted by models (Kring and Durda 2002). The maximum phase of dust remobilisation occurred at the paroxysm of the 4 kyr BP event and persisted for some years due to the fragility of the soil-landscapes before the regeneration of the soil cover was completed. The occurrence of glass shards typical of the 4 kyr BP exotic assemblage (Cullen et al. 2000) confirms that the spike from core M5−422 in the Arabian Gulf can be assigned to the distinctive 4 kyr BP dust. The absence of a similar dust spike in core 905 offshore near Somalia, considered to provide a high resolution record of dust flux during the Holocene (Jung et al. 2004), would support a spatially variable dust re-mobilisation.

The regional manifestation of the dust event would possibly depend upon the availability of the dust sources over the destabilised lands, the directions of the windstorm tracks from land to ocean, as well as spatial variability of the impact-ejecta dispersion. The misinterpretation of the overlapping radiometric dates for core M5–422 would explain how a real short-term dust event was transformed by Cullen et al. (2000) into an erroneous 300 years long mega-drought. In addition, the lack of detailed characterization of the dust assemblage does not exclude reworking by bottom currents of the original 4 kyr BP micro-debris. Vertical dispersion of the micro-debris would be easily confused with a dust event of long duration, unless the integrity of the dust record is securely established.

The sequence of pedo-sedimentary events following the 4 kyr BP abrupt event expresses: (i) direct effects of the impact-ejecta delivery processes, in particular the burning, the air blast and the atmospheric dust loading and (ii) indirect consequences of the dust-fallout-related disruption of soil-landscape stability.

The important variations in intensity and duration of the environmental disturbances between the three regions studied reflect their intrinsic resilience. Therefore, the sequence of pedo-sedimentary events identified in the three regions studied does not show at around 4 kyr BP any other environmental change than the ones initially triggered by the 4 kyr BP impact-ejecta event.

In contrast to the widely accepted occurrence of a rapid climate change during the 4200–3800 yr BP time interval (Mayewski et al. 2004), we propose that the widespread pronounced environmental changes recorded at about 4 kyr BP correspond to the direct and indirect consequences of the 4 kyr BP impact-ejecta fallback. This distinctive event might have exerted an influence on the global climate, in particular through injection in the upper atmosphere of volatile components and carbon-rich aerosols, known to induce cloud condensation nuclei effects and albedo changes (Toon et al. 1997).

6 Conclusions

This comparative study of the 4 kyr BP event in different regions demonstrates that soil micro-fabrics are reliable archives to reconstruct the timing of environmental perturbations induced over wide areas. Similar to the leading role played by high resolution records from deep sea, lake, and ice cores, soil sequences where rapid burial has allowed the exceptional preservation of a high quality signal appear to be of major interest. These peculiar situations offer a unique opportunity to discriminate the instantaneous soil reactions directly triggered by unusual phenomena such as a cosmic collision or any other internal cause, from the more long-term indirect effects on soil landscapes.

As illustrated by data from NE Syria, the possibility to capture high quality signals, in a wide diversity of local conditions in cumulative soil landscapes, is essential to appreciate both the spatial diversity inherent in the involved phenomena, and the spatial variability of soil responses with respect to the local factors. These ideal situations provide interpretative keys to approach the more fragmentary records available from the great majority of regions. These relict signals would be easily confused with human-induced perturbations (i.e. the 4 kyr BP signal in West France), or with a gradual climate change (i.e. the 4 kyr BP signal in the Moche valley) or with a recurrent erosional crisis (i.e. the 4 kyr BP signal in the Vera basin).

Although of different quality, data retrieved from a large variety of regions should help to finally understand a global event throughout its spatial complexity.

Acknowledgements Our deep thanks are addressed to those involved in this project who contributed to solving the puzzle of the 4 kyr BP event: Hélène Cachier, Tyrone Daulton, François Guichard, Eric Leroy, Jean-Louis Pastol, Bernhard Peucker-Ehrenbrink, Greg Ravizza, Franck Poitrasson, Gérard Sagon, Urs Schärer, Alex Shukolyukov, and Michael Walls. The detailed analytical characterization of the impact signal will be presented elsewhere.

We are greatly indebted to all those who have facilitated our access to the materials used in this Chapter: Harvey Weiss and Bertille Lyonnet for NE Syria; Vincente Lull and his team for the Vera basin; Claude Chauchat and Santiago Uceda for the Moche valley Peru; and Claude Burnez and Catherine Louboutin at Ebeon (France).

Nicolas Fedoroff and Stéphane Gaffié are gratefully acknowledged for their support in the field and in the laboratory.

References

Alley RB, Meese DA, Shuman CA, Gow AJ, Taylor KC, Grootes PM, White JWC, Ram M, Waddington ED, Mayevski PA, Zielenski GA (1993). Abrupt increase in snow accumulation at the end of the Younger Dryas event. Nature 362: 527–529

Almendros G, Gozales-Vila FJ, Martin F (1990) Fire-induced transformation of soil organic matter from an oak forest: An experimental approach to the effects of fire on humic substances. Soil Sci 49 (3): 158–168

Bond GC, Showers W, Elliot M, Evans M, Lotti R, Hajdas I, Bonani G, Johnson S (1999) The North Atlantic's 1–2kyr climate rhythm: Relation to Heinrich events, Dansgaard/Oeschger cycles and the little ice age. In: Clark PU, Webb RS, Keigwin LD (eds.) Mechanisms of Global Climate Change at Millennial Time Scales. Am Geophys Union Geophys Monogr, Washington DC 112: 35–58

Bullock P, Fedoroff N, Jongerius A, Stoops G, Tursina T, Babel U (1985) Handbook for Soil Thin Section Description, Waine Research Publications, Wolverhampton, UK

Burnez C, Fuoueré P (1999). Les enceintes néolithiques de Diconche (Saintes, Charente-Maritime). Poitiers, 1999 (Mémoire XV)

Courty MA (1994) Le cadre paléogéographique des occupations humaines dans le bassin du Haut Khabour (Syrie du nord-est). Premiers résultats. Paléorient 20(1): 21–59

Courty MA (1998) The soil record of an exceptional event at 4000 B.P. in the Middle East. In: Peiser BJ, Palmer T, Mailey ME (eds.) Natural Catastrophes During Bronze Age Civilisations. Archaeological, ecological, astronomical and cultural perspectives. BAR Inter Series 728: 93–108

Courty MA (2001) Evidence at Tell Brak for the Late ED III/Early Akkadian Air Blast Event (4 kyr BP). In: Oates D, Oates J, McDonald H (eds.) Excavations at Tell Brak, Vol. 2: Nagar in the Third Millennium B.C. McDonald Institute Monographs, Cambridge, UK

Courty MA (2003) Tracing the 4 kyr BP dramatic event in soils and archaeological sediments across the Near East. In de Merocheji P, Thalman JP, Margueron JC (eds.) Actes du 3ème Congrès International d'Archéologie du Proche Orient, Paris

Courty MA, Goldberg P, Macphail RI (1989) Soil, Micromorphology and Archaeology. Cambridge Manuals in Archaeology, CUP, Cambridge

Courty MA, Fedoroff N, Jones MK, Castro P, McGlade J (1995) Environmental dynamics. In: Van der Leeuv S (ed.) Understanding the Natural and Anthropogenic Causes of Soil Degradation and Desertification in the Mediterranean Basin. The Archaeomedes project. Final Report of the contract EV5V-0021 for the Directorate General XII of the Commission of the European Union

Courty MA, Fedoroff M, Greenwood P, Grice K, Guichard F, Mermoux M, Schärer U, Shukolyukov A, Smith DC, Thiemens MH (2005) Formative processes throughout lands and seas of the 4-kyr BP impact signal. SEPM Research Conference. In: The Sedimentary Record of Meteorite Impacts. Springfield, Missouri, USA

Courty MA, Deniaux B, Crisci A, Fedoroff M, Greenwood P, Grice K., Mermoux M, Schärer U, Shukolyukov A, Smith DC, Thiemens MH (2006) High resolution soil records of impact-ignited fires at 4 kyr BP in various regions of the Near East, West Europe and Peru. Geophys Res Abs 8:33–78

Cullen HM, de Menocal PB, Hemming S, Hemming G, Brown FH., Guilderson T, Sirocko, F (2000) Climate change and the collapse of the Akkadian Empire. Evidence from the deep sea. Geology 28: 379–382

de Menocal P (2001) Cultural responses to climate change during the late Holocene. Science 292: 667–673

Gaffie S, Bruand A, Courty MA (2001) Analyse de la microstructure d'un horizon de surface enterré sous des matériaux archéologiques du Bronze Ancien en Syrie (2200 BC). CR Acad Sci Série II 332: 153–160

Giovannini G, Lucchesi S, Cervelli S (1983) Water-repellent substances and aggregate stability in hydrophobic soil. Soil Sci 135(2): 110–113

Graup G (1999) Carbonate-silicate immiscibility upon impact melting: Ries crater, Germany. Meteorit Planet Sci 34: 425–438

Heimann R (1982) Firing technologies and their possible assessment by modern analytical methods. In: Olin JS, Franklin AD (eds.), Archaeological Ceramics, Smithsonian Institution Press, Washington, DC

Hubbert KR, Preisler HK, Wohlgemuth PM, Graham RC, Narog MG (2006) Prescribed burning effects on soil physical properties and soil water repellency in a steep chaparral watershed, southern California, USA. Geoderma 130: 284–298

Humbert L (1972) Atlas de pétrographie des systèmes carbonatés. Technip, Paris

IUSS Working Group, WRB (2006) World reference base for soil resources. 2nd edition. World Soil Resources Reports 103. FAO, Rome

Jung SJA, Davies GR, Ganssen GM, Kron D (2004) Stepwise Holocene aridification in NE Africa deduced from dust-borne radiogenic isotope records. Earth Planet Sc Lett 221: 27–27

Kieffer SW (1977) Impact conditions required for formation of melt by jetting in silicates. In: Roddy, DJ, Pepin RO, Merrill RB (eds.) Impact and Explosion Cratering. Pergamon, New York

Kring DA (1997) Air blast produced by the Meteor Crater impact event and a reconstruction of the affected environment. Meteorit Planet Sci 32: 517–530

Kring DA, Durda DD (2002) Trajectories and distribution of material ejected from the Chicxulub impact crater: Implications for post-impact wildfires. J Geophys Res 107(E6) 10 1029/2001JE0011532

Marchant R, Hooghiemstra H (2004) Rapid environmental changes in African and South American tropics around 4000 years before present: A review. Earth-Sci Rev 66: 217–260

Mayewski PA, Rohling EE, Stager JC, Karlen W, Maasch KA, Mekk LD, Meyerson EA, Gasse F, van Kreveld S, Holmegren K, Lee-Thorp J, Rosquist G, Rack F, Staubwasser M, Shneider RR, Steig EJ (2004) Holocene climate variability. Quaternary Res 62:242–255

Ott d'Estevou Ph, Montennat C, Alvadao C (1990) Le bassin de Vera – Garrucha. In: Montenat C (ed) Documents et travaux de l'IGAL, Paris

Pavlik RS, Holland HJ, Payzant EA (2001) Thermal Decomposition of Zircon Refractories. J Am Ceram Soc 84 (12): 2930–2936

Scott DF, Van Wyk DB (1990) The effect of wildfire on soil wettability and hydrological behaviour of an afforested catchment. J Hydrol 121: 239–256

See TH, Wagstaff J, Yang V, Horz F, MacKay GA (1998) Compositional variation and mixing of impact melts on microscopic scales. Meteorit Planet Sci 33(4): 937–948

Soil Survey Staff (1993) Keys to Soil Taxonomy. US Department of Agriculture Natural Conservation Service. 9th edition, Washington DC.

Thompson L, Mosley-Thompson N, Davis ME, Henderson KA, Brecher HH, Zagorodnov, VS, Mashiotta T, Lin PN, Mikhalenko V, Hardy DR, Beer J (2002) Kilimanjaro ice core records: Evidence of Holocene climate change in Tropical Africa. Science 298: 589–593

Toon OB, Zahnle K, Morrison RP, Turco R, Covey C (1997) Environmental perturbations caused by asteroid impacts. Rev Geophys 35: 41–78

Wang S, Zhou T, Cai J, Zhu J, Xie Z, Gong D (2004) Abrupt climate change around 4 ka BP: Role of the thermohaline circulation as indicated by GCM experiment. Adv Atmos Sci 21(2): 261–295

Weiss H (2001) Beyond the Younger Dryas. Collapse as adaptation to abrupt climate change in ancient West Asia and the Eastern Mediterranean. In: Bawden G, Reycraft RM (eds.) Environmental disaster and the Archaeology of Human Response. Maxwell Museum of Anthropology, Albuquerque, NM. Anthropological papers 7: 75–98

Weiss H, Courty MA, Wetterstrom W, Meadow R, Guichard F, Senior L, Curnow A (1993) The origin and collapse of Third Millennium North Mesopotamian Civilisation. Science 261: 995–1004

Weiss H, Bradley RS (2001) What drives societal collapse? Science 291:609–610

Zazo C, Goy JL, Dabrio CJ, Bardaji T, Somoza L, Silva PG (1993) The last Interglacial in the Mediterranean as a model for the present Interglacial. Global Planet Changes 7: 109–117